



## Characteristics of common-mode conducted emission of multi-boost converters

Muhammad Imam Sudrajat<sup>a, b, \*</sup> , Afiva Riyatun Nuvus<sup>c</sup>, Dwi Mandaris<sup>a</sup> 

<sup>a</sup> Research Center for Testing Technology and Standards, National Research and Innovation Agency (BRIN) Kawasan Sains dan Teknologi (KST) Bacharuddin Jusuf Habibie, Jalan Raya Puspiptek 60, Tangerang Selatan, 15310, Indonesia

<sup>b</sup> Faculty of Electrical Engineering, Mathematics and Computer Science, University of Twente Drienerlolaan 5, Enschede, 7522 NB, The Netherlands

<sup>c</sup> Faculty of Mathematics and Natural Sciences, Universitas Negeri Jakarta Gedung Hasjim Asj' arie Kampus A, Jalan Rawamangun Muka, Jakarta, 13220, Indonesia

Received 28 August 2023; Revised 24 November 2023; Accepted 4 December 2023; Published online 29 December 2023

### Abstract

One of the primary challenges faced when utilizing power converters such as a DC boost converter is electromagnetic interference (EMI) issues, one of which is common-mode (CM) noise. In order to mitigate the unwanted EMI from converters and design proper EMI filters, it is imperative to possess comprehensive insight into the characteristics of CM noise generated from the converters. This study presents the investigation regarding the characteristic of CM noise emitted by multi-boost converters when operated under varying duty cycle conditions. The research was conducted by measuring and analyzing the CM noise generated by three identical boost converters arranged in a parallel configuration. The result shows that the amplitude of each harmonic of CM noise generated by the multi-boost converters is 5 dB to 10 dB higher than CM noise from a single-boost converter. This is due to each converter being configured in the same conditions, producing a constructive interaction of the generated CM noise. Moreover, the duty cycle of pulse-width modulation (PWM) has a strong influence on the characteristic of the amplitude of each harmonic frequency. It is proven by the amplitude pattern of each harmonic of CM noise. Under duty cycle variations, the converters generate similar peaks and valley amplitude patterns as the Fourier transformation of the trapezoidal waveform used in the PWM setting.

Copyright ©2023 National Research and Innovation Agency. This is an open access article under the CC BY-NC-SA license (<https://creativecommons.org/licenses/by-nc-sa/4.0/>).

Keywords: common-mode (CM) noise; duty cycle; electromagnetic interference (EMI); multi-boost converters; pulse-width modulation (PWM).

### I. Introduction

The emphasis on enhancing energy efficiency and reducing CO<sub>2</sub> levels has led to the utilization of energy-saving equipment. In response to this requirement, switching-based power converters such as DC-DC converters, AC-DC converters, and inverters are now widely used in many applications such as in light-emitting diode (LED) lamps, switch-mode power supply (SMPS), motor drives, and electric vehicle charging systems. Compared to conventional voltage dividers, switching-based converters offer more advantages, such as minimized power dissipation, greater flexibility, and reduced voltage drop.

However, due to high  $dV/dt$  voltages and high  $dI/dt$  current in the circuit during the fast-switching mechanism, utilization of a power converter can lead to adverse consequences, specifically in the form of electromagnetic interference (EMI) [1][2][3]. Moreover, interferences from an EMI source, such as a converter, can propagate and disturb the performance of the other electrical equipment and cause signal integrity (SI) problems [4]. EMI noise generated from switching-based equipment is also the main factor that can degrade a power system's power quality and cause motor overvoltage [5]. Interference between sources and victims occurs when the frequency of an unwanted signal is within the intermediate frequency (IF) bandwidth of a victim's operating frequency [6]. Interference between sources and victims may also occur from intermodulation distortions, where multiple signals

\* Corresponding Author. Tel: +62-85280835553  
E-mail address: muha096@brin.go.id

are combined. Moreover, the coupling path of interference can be through radiation or conduction [7]. EMI noise propagating through air or vacuum is termed radiated emission (RE), and EMI noise propagating through conductive material is termed conducted emission (CE). Figure 1 shows the mechanism of interference between sources and victims.

In the case of CE from a converter, high  $dV/dt$  voltage transient during the “off” to “on” states or vice versa generate high-frequency noise on the frequency domain. This noise can propagate through conducted material such as cable, heatsink, casing, or parasitic capacitance between two conductive materials [8]. In a complex system without a proper grounding system, such as an islanded microgrid, this noise can interfere with other systems or subsystems that are located far away from the source [8][9].

Based on their path, CE is divided into two types: differential mode (DM) and common-mode (CM) [2]. DM noise refers to signals that flow through two different conductors at the same time but in the opposite direction. DM represents the different potential between two conductors. DM mostly relates to the additional transmitted data or signal delivered through the conductors. In many cases, DM is expected and normally occurs. However, without proper mitigation, the DM signal can also be noise to other systems. On the other hand, CM noise refers to noise signals that flow through two different conductors at the same time and in the same direction. When there is a parasitic capacitance, the potential difference between the two conductors and the ground or the reference will cause a ground CM loop [3][10][11].

This interference occurs at the fundamental frequency of the switching mechanism and harmonic frequencies [12]. For example, conducted EMI from DC-DC converters often causes power quality problems in microgrids and electric or hybrid vehicles [13]. EMI can never be eliminated; however, it can be mitigated and suppressed by installing a filter, ferrite, or shielding. Nonetheless, to design a proper EMI filter, accurate information related to the characteristics of EMI generated from the source is required. Moreover, understanding EMI characteristics is essential to determine limitations or operating procedures to avoid excessive emissions and to meet relevant electromagnetic compatibility (EMC) standards.

The characteristics and spectrum profile of CE noise generated from a converter are greatly influenced by its operational condition, particularly the setting of the pulse-width modulation (PWM) such as rise time ( $\tau_r$ ), switching frequency ( $f_{sw}$ ) [14][15] and duty cycle ( $D$ ) [16][17]. In addition, the application of more than one converter in a system has a greater risk of generating higher EMI, especially if the EMIs have a constructive signal interaction. Research on multi converters by [14][15] discover the effect of variation of switching frequency on EMI level. Multi converters with random modulation (random switching frequency) PWM, tend to generate relatively lower EMI noise

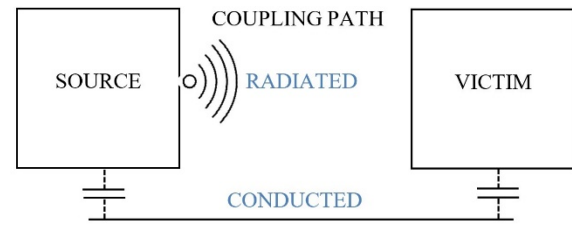


Figure 1. EMI mechanism

levels compared to the EMI produced by converters with deterministic modulation (constant switching frequency) setting. It happens because the EMI power from the converters is spread over the frequency range [15]. Unfortunately, the information about the CE spectrum characteristics of the multi-converters cannot be fully explained in [14][15] because it is only focused on the effect of switching frequency, while the effect of duty cycle has not been explored yet due to the setting of duty cycle used in these studies is constant ( $D = 50\%$ ). Meanwhile, in the real application, most converters will be operated under the various values of the duty cycle to obtain the desired level.

Furthermore, the effect of duty cycle variation on CE has been studied by [16][17]. The result shown in [16][17], implies that the level of CE noise from a single DC boost converter is very influenced by the converter’s PWM duty cycle setting. However, these studies only observe the CM characteristics of a single boost converter, whereas, in a complex system such as a microgrid, several converters are often installed in parallel to meet the needs of the installed loads [18]. There is a gap in the existing literature that describes in detail the characteristics of the CM behavior generated by multi-boost converters under duty cycle variations. To address this gap, the main purpose of this study is to obtain the CM characteristics of multi-boost converters, particularly the CM noise generated from the simultaneous operation of multi-boost converters. In this study, the scope of the investigation is focused on the adjustable DC boost converters arranged in a parallel configuration. Investigation into other types of converters, as well as their combinations, will be carried out in future research.

## II. Materials and Methods

### A. Design of adjustable multi-boost converters

A boost converter is a power converter that aims to increase the output voltage above the input voltage. A boost converter is normally installed in an LED lamp, a power supply, an uninterruptible power supply (UPS), or in a renewable power system. The voltage regulation of the boost converter is done by controlling the time the switch remains “on” and “off” during each switching cycle. This cycle is correlated with the duty cycle and switching frequency of the PWM signal. The boost converter’s output voltage can be calculated using equation (1) to equation (3).

$$V_{out} = \frac{V_{in}}{1-D} \quad (1)$$

$$D = \frac{\tau}{T} \times 100\% \quad (2)$$

$$T = \frac{1}{f_{sw}} \quad (3)$$

where  $V_{in}$  is the DC input voltage (V),  $V_{out}$  is the DC output voltage (V),  $D$  is the duty cycle (%),  $\tau$  is the time when the pulse remains "on" (s),  $T$  is the cycle period (s),  $f_{sw}$  is the switching frequency (Hz),  $\tau_r$  is the rise time (s), and  $\tau_f$  is the fall time (s). In real conditions, the shape of PWM pulses cannot be perfect as a square pulse but in the shape of trapezoidal pulses, which have a finite  $dV/dt$ . Figure 2 and Figure 3 show the general schematic of a boost converter and the trapezoidal pulse of the PWM waveform.

Furthermore, through the Fourier transformation, the amplitude of each harmonic spectral of a trapezoidal waveform can be expressed as equation (4),

$$A_{km} = 2V_{in} \frac{\tau}{T} \left| \frac{\sin(k\pi\frac{\tau}{T})}{k\pi\frac{\tau}{T}} \right| \left| \frac{\sin(k\pi\frac{\tau_r}{T})}{k\pi\frac{\tau_r}{T}} \right| \quad (4)$$

where  $A_{km}$  is the amplitude of each harmonic (dBV) and  $k$  represents the  $n^{\text{th}}$  harmonic.

In this study, the PWM pulse is controlled by Arduino Uno through its analog ports. Three boost converters have identical designs and layouts are developed. They have the same configuration and component value. An independent PWM input controls every boost converter through a separate Arduino analog port. This PWM pulse from Arduino controls the "on" and "off" conditions of the transistor gate [19]. In this study, the utilized PWM mode for each converter is deterministic modulation, in which every PWM pulse has constant switching frequency [20]. In this study, the switching frequency of each boost converter is set to 20 kHz. The duty cycle of each boost converter is varied between 10% to 80%. The observation is limited to  $D = 80\%$  due to the excessive heating generated by the MOSFET. The duty cycle is adjusted via Arduino's code by setting the "PWM setting" variable, where 255 represents the maximum value or PWM = 100 %, as shown in equation (5). For instance, to achieve a duty cycle of 50 %, a value of 127 is inputted into the Arduino code.

The value of each component of the boost converter is determined based on a calculation to avoid over-peak-to-peak ripple current in the inductor ( $L$ ) and over-peak-to-peak ripple voltage on the capacitor ( $C$ ). The rule of thumb to determine the value of the ripple current is 10% to 30% of the input current, and the ripple voltage is 1% to 5% of the output voltage. The inductance value is calculated based on equation (6), and the capacitor value is calculated based on equation (7), where  $L$  is the inductance value (H),  $I_{ripple}$  is the maximum current ripple expected (A),  $I_o$  is the maximum output current (A),  $C$  is the capacitance value (F), and  $V_{ripple}$  is the maximum voltage ripple expected (V).

$$D = \frac{\text{PWM setting}}{255} \times 100\% \quad (5)$$

$$L = \frac{V_{in} D}{f_{sw} I_{ripple}} \quad (6)$$

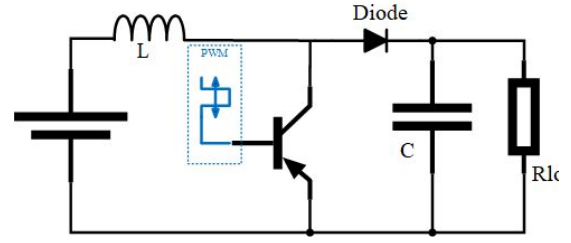


Figure 2. Schematic of a boost converter

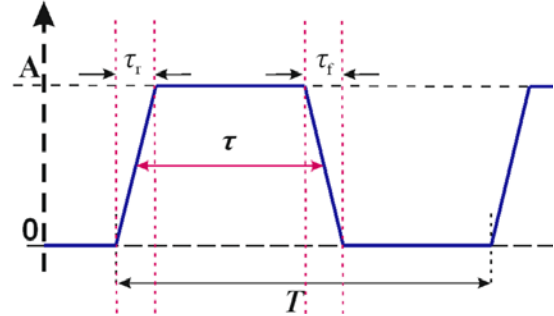


Figure 3. Trapezoidal pulse of PWM

Table 1.  
Components of the boost converter

Component	Type or Value
Transistor	MOSFET IRF540N
Diode	1N4007
Inductor	100 $\mu$ H
Capacitor	10 $\mu$ F
Resistor load	220 $\Omega$

$$C = \frac{I_o D}{f_{sw} V_{ripple}} \quad (7)$$

In developing the boost converter, the authors first simulate the design using SPICE software to ensure that the boost converter can perform properly and has acceptable ripple voltage and current voltage. The schematic is then transferred to a through-hole printed circuit board (PCB) dot matrix. The inductor and capacitor installed on the PCB are an inductor and a capacitor on the market that have a value close to the value calculated by equation (6) and equation (7). Each boost converter has the same component value, load, and layout. The components utilized in the boost converter circuit are shown in Table 1.

## B. Measurement setup

This study observed CM noise characteristics from a multi-boost converter using an Agilent N9038A EMI receiver and a pair of TBL0550-1 DC line impedance stabilization networks (LISN) from TekBox®. The converters are supplied by 9 VDC from a programmable DC voltage supply. Installing a pair of LISNs between the DC power supply and the converters aims to filter unwanted noise originating from the programmable DC power supply and also to match the impedance. This ensures that the receiver only captures CM noise from the converters. Inside the LISN, the CM current ( $I_{CM}$ ) flows through the standardized 50  $\Omega$  impedance. The LISN mate compiles the CM voltage ( $V_{CM}$ ) from both LISNs then the voltage value is processed and displayed by the EMI receiver. The schematic and the layout of the

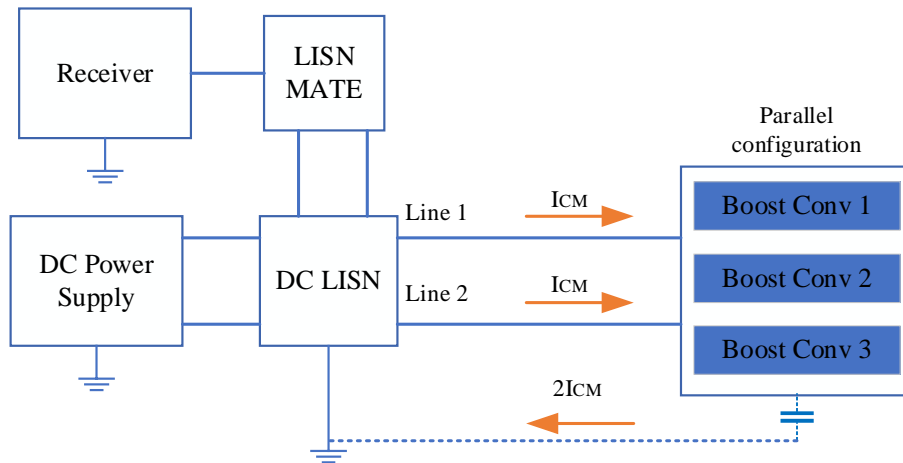


Figure 4. Schematic of the CM measurement

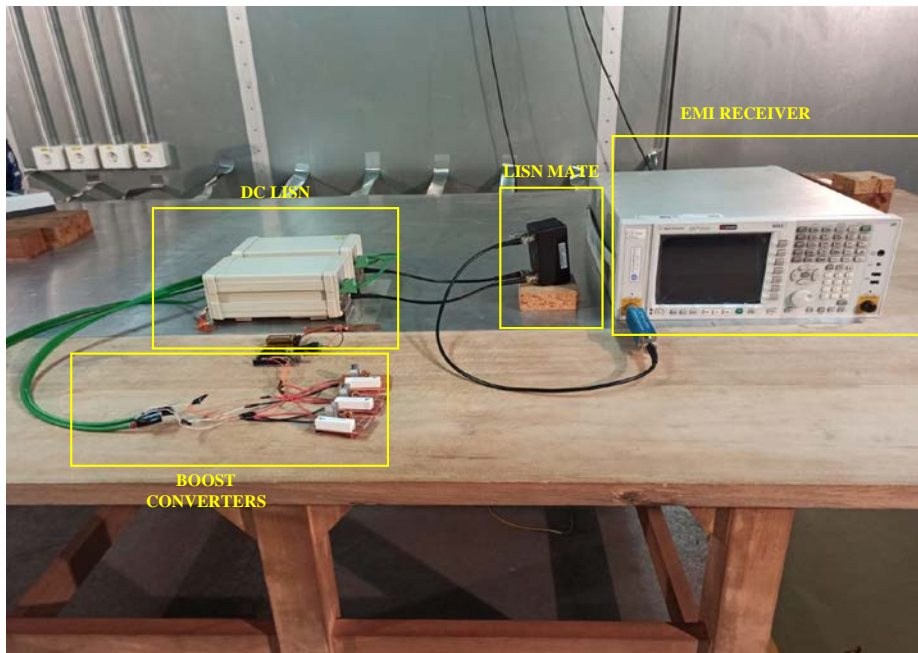


Figure 5. CM measurement setup

measurement are shown in Figure 4 and Figure 5. Since the TBL0550-1 does not have any protective element in the radio frequency (RF) path and to prevent damage to the receiver, a 10 dB attenuator is added to the RF path. Moreover, to get a detailed value and pattern of the CM noise amplitude, the observation is only focused on the frequency range of 20 kHz to 200 kHz.

In general, noise floor, cable type, length, equipment configuration under test (EUT) and layout, LISN, PWM setting ( $\tau_r$ ,  $f_{sw}$ , and  $D$ ), loads, and uncertainty factors could affect the level of CM spectrum. However, the experiment was done in the standard shielded well-grounded room to ensure that the outside EMI noise does not affect the measurement results. Furthermore, this study is focused on the effect of the duty cycle variation on CM noise characteristics; thus, factors other than the duty cycle are kept constant during the measurement. The deterministic PWM structure of the Arduino's code that is applied to control the converter output voltage is developed based on equation (4). In each of these measurements, all

converters are set to the same duty cycle value, which ranges from 10% to 80%. The final data recorded by the EMI receiver and then being analyzed using MATLAB<sup>®</sup>. Each dBuV value of fundamental frequency and its harmonic under the variation of the duty cycle is recorded and then plotted in  $x$ - $y$  graphs.

### III. Results and Discussions

Figure 6 shows that the spectrum of CM noise is significantly impacted by the switching frequency of PWM. This is evident from the noise present at the fundamental frequency (20 kHz) and its harmonics, which 20 kHz is the switching frequency of the PWM. Moreover, Figure 6 also indicates that the level of CM noise increases with the increasing number of installed converters. CM noise from the triple converter is 5 dB to 10 dB higher than the single converter. This is due to the multi-boost converters with the same PWM setting operating in parallel, and the overall current demands drawn from the power supply are increased. This leads to higher current-related noise that couples into the CM loop.

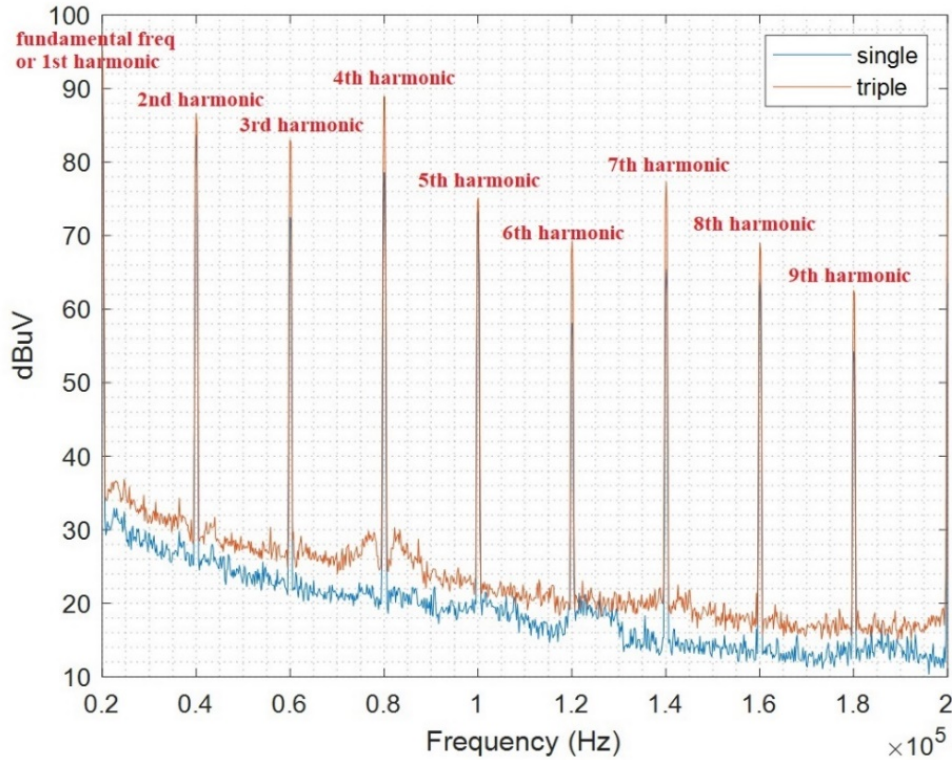


Figure 6. CM spectrum of single converter and triple converter at duty cycle of 60 %

Thus, the current flowing through the  $50\ \Omega$  resistor LISN node is the accumulation of the current that flows from each converter branch, and this result is in accordance with Kirchhoff's law. In practice, the more converter with the same duty cycle value installed on the system, the greater the potential for interference.

Furthermore, related to the effect of the duty cycle variation, there is a different behavior pattern of the amplitude of each CM harmonic signal. The behavior of the CM noise generated at the fundamental frequency (20 kHz) shows a semi-parabolic pattern when the duty cycle is increased. Based on the measurement result, at the fundamental frequency (20 kHz), the highest CM noise occurs at the duty cycle of between 50% to

80%. Figure 7 shows the behavior of the CM noise of the fundamental frequency under duty cycle variation. A different pattern is shown by CM noise at the 2<sup>nd</sup> harmonic (40 kHz). There are two peaks between 25% to 35% and 75% to 80% of the duty cycle. Contrary to the fundamental frequency, CM noise at the duty cycle of 50% of the 2<sup>nd</sup> harmonic is very low. It happens not only at the observation of the single converter but also at the triple converter. In this study, it is stated as "peaks" and "valleys" referred to [16]. The CM noise of the 3<sup>rd</sup> harmonic also shows peak and valley patterns, the peaks occur between 15% to 20%, 50% to 60%, and 80%. The behavior of the CM noise of the 2<sup>nd</sup> harmonic, the 3<sup>rd</sup> harmonic, and the 4<sup>th</sup> harmonic are shown in Figure 8.

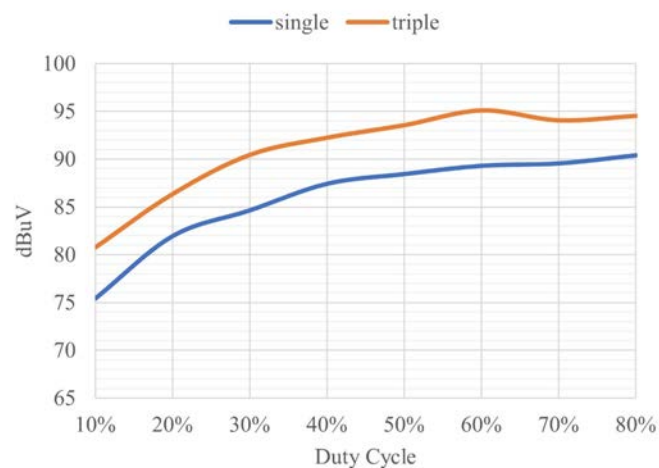


Figure 7. Pattern of the CM noise amplitude of the fundamental frequency

This “peaks and valleys” pattern is distinctive because it closely resembles the pattern generated by the Fourier transformation of the trapezoid-shaped pulse used by PWM control. As shown in Figure 9, plotting equation (4) results in a similar pattern as obtained from the measurement. The appearance of this pattern has highlighted the

evidence that the pulse shape of PWM particularly the setting of the duty cycle has a significant impact on the characteristic of CM noise of multi-boost converters. Regarding the EMI mitigation measures, the engineers can use this pattern as a useful tool to predict and avoid operating multi-boost converters on the highest CM noise.

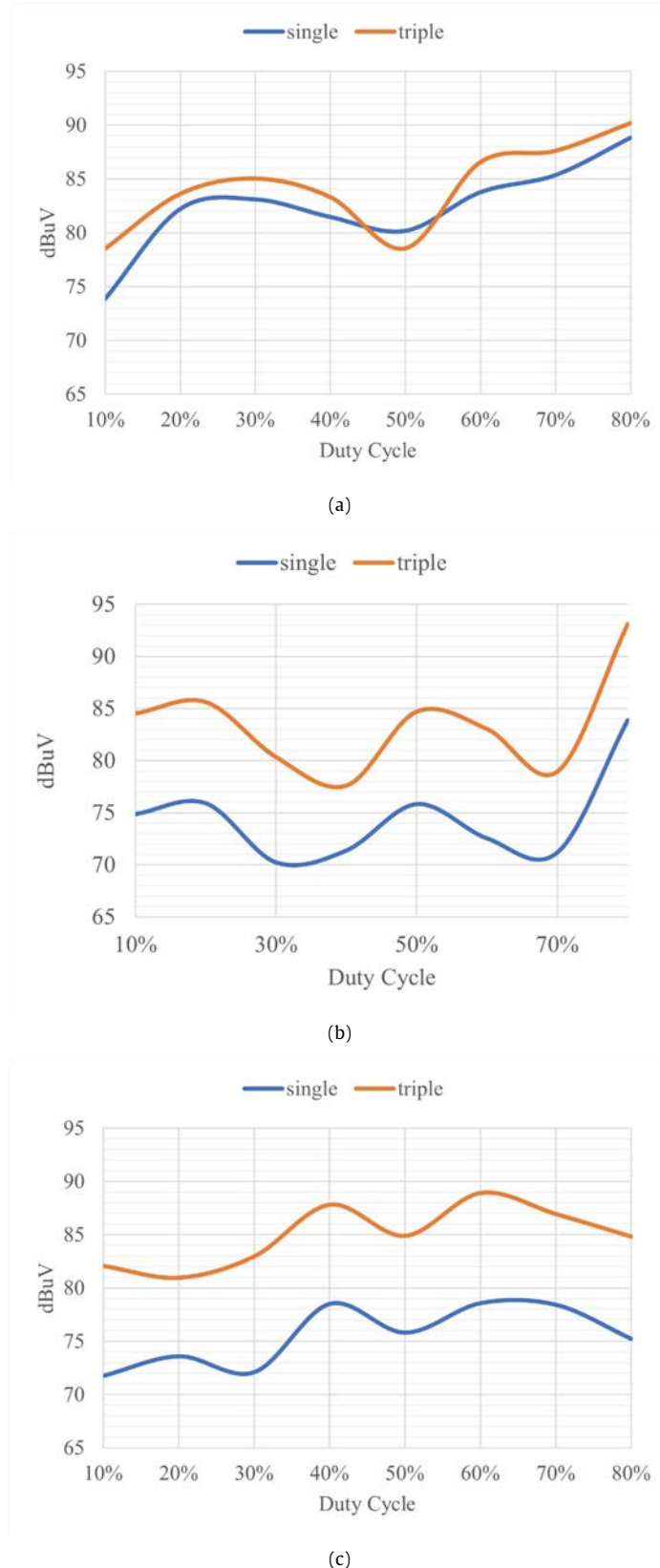


Figure 8. Pattern of the CM noise amplitude of the: (a) 2<sup>nd</sup> harmonic; (b) 3<sup>rd</sup> harmonic; (c) 4<sup>th</sup> harmonic

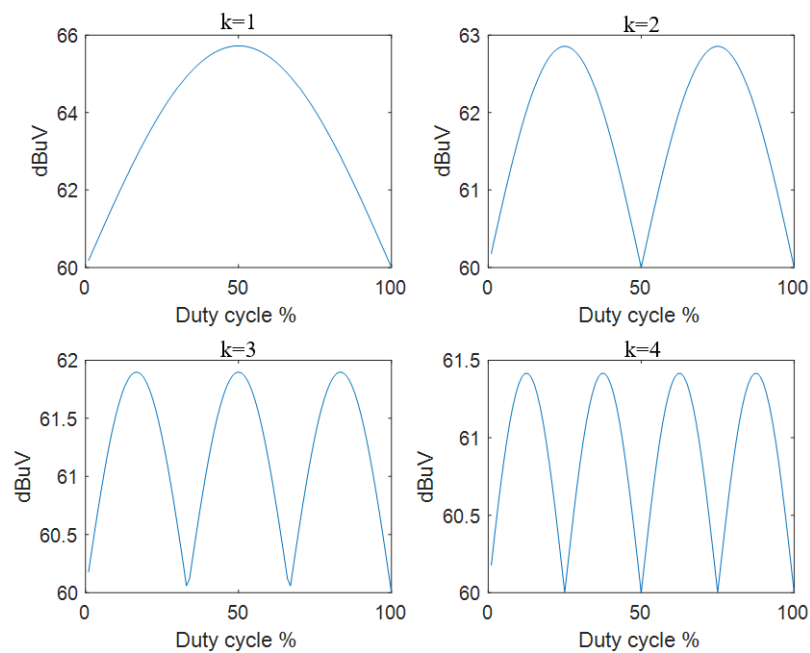


Figure 9. Pattern obtained from equation (4)

## IV. Conclusion

The objective of this study was to understand the characteristics of CM of multi-boost converters under duty cycle variation. The investigation concludes that the number of converters can significantly affect the level of CM noise. Installing more converters in parallel with the same duty cycle setting can increase the CM noise in the system. This is proven by the experiment, which found that CM noise from the three converters generates 5 dB to 10 dB higher than the single converter. The investigation also revealed that the amplitude level of the fundamental frequency and its harmonic is affected by the trapezoidal pulse employed on PWM control. The duty cycle in the PWM setting will affect the amplitude level of CM noise of the fundamental frequency and its harmonics. Under duty cycle variation, the pattern of CM noise amplitude is in the form of "peaks" and "valleys". With the same duty cycle variation setting, the CM noise pattern generated from the multi-boost converters also shows a similar pattern but has a higher level. This occurs due to a constructive interaction of the CM noise when each converter is set with the same conditions. This pattern proves that the duty cycle setting strongly influences the CM noise. The investigation of this study suggests that it is possible to predict the characteristics of CM noise of DC converters based on the shape of their PWM pulse. The "peaks" and "valleys" pattern as the effect of PWM duty cycle variation can be used to avoid the worst EMI generated by multi-boost converters. This work has opened several questions that need further investigation. Further work needs to be done to establish whether setting different duty cycle values of each converter at the same time can debilitate mutually the CM level. Furthermore, by knowing the characteristics of CM noise, the EMI mitigation process can be carried out more easily.

## Acknowledgements

The authors would like to thank Indrasari, Widyaningrum for her support regarding the collaborative program between the National Research and Innovation Agency (BRIN) and Universitas Negeri Jakarta.

## Declarations

### Author contribution

All authors contributed equally as the main contributor of this paper. All authors read and approved the final paper.

### Funding statement

This research did not receive any specific grant from funding agencies in the public, commercial, or not-for-profit sectors.

### Competing interest

The authors declare that they have no known competing financial interests or personal relationships that could have appeared to influence the work reported in this paper.

### Additional information

Reprints and permission: information is available at <https://mev.brin.go.id/>.

Publisher's Note: National Research and Innovation Agency (BRIN) remains neutral with regard to jurisdictional claims in published maps and institutional affiliations.

## References

- [1] J. Qu, Q. Zhang, Y. Wang, and S. Cui, "Conducted EMI Investigation of a SiC-Based Multiplexing Converter for EV/PHEV," *IEEE Access*, vol. 9, pp. 58807–58823, 2021.
- [2] T. J. Donnelly, S. D. Pekarek, D. R. Fudge, and N. Zarate, "Thévenin Equivalent Circuits for Modeling Coupled Common/Differential-Mode Behavior in Power Electronic Systems," *IEEE Open Access Journal of Power and Energy*, vol. 8, pp. 377–388, 2021.

- [3] J. C. Helton, A. N. Lemmon, and A. D. Brovont, "Comprehensive Analysis of Filter Inductor Topology on Common-Mode Conducted Emissions for the Boost Converter," *IEEE Trans Power Electron*, vol. 38, no. 4, pp. 4647–4657, Apr. 2023.
- [4] E. Serban, C. Pondiche, and M. Ordenez, "Analysis and Design of Bidirectional Parallel-Series DAB-based Converter," *IEEE Trans Power Electron*, vol. 38, no. 8, pp. 10370–10382, 2023.
- [5] Y. Xu et al., "Impact of High Switching Speed and High Switching Frequency of Wide-Bandgap Motor Drives on Electric Machines," *IEEE Access*, vol. 9, pp. 82866–82880, 2021.
- [6] A. Gharib, H. D. Griffiths, and D. J. Andrews, "Prediction of Topside Electromagnetic Compatibility in Concept-Phase Ship Design," *IEEE Trans Electromagn. Compat.*, vol. 59, no. 1, pp. 67–76, Feb. 2017.
- [7] Z. Zhang, Y. Hu, X. Chen, G. W. Jewell, and H. Li, "A Review on Conductive Common-Mode EMI Suppression Methods in Inverter Fed Motor Drives," *IEEE Access*, vol. 9, pp. 18345–18360, 2021.
- [8] A. D. Brovont, A. N. Lemmon, C. New, B. W. Nelson, and B. T. Deboi, "Analysis and Cancellation of Leakage Current through Power Module Baseplate Capacitance," *IEEE Trans Power Electron*, vol. 35, no. 5, pp. 4678–4688, May 2020.
- [9] M. I. Sudrajat, N. Moonen, H. Bergsma, R. Bijman, and F. Leferink, "Multipoint measurement technique for tracking electromagnetic interference propagation and correlation in a complex installation," in *2020 IEEE International Symposium on Electromagnetic Compatibility, Signal Integrity and Power Integrity*, Reno, NV, USA: IEEE, Sep. 2020.
- [10] R. Phukan, X. Zhao, P. Asfaux, D. Dong, and R. Burgos, "Investigation of Staggered PWM Scheme for AC Common Mode Current Minimization in SiC-Based Three-Phase Inverters," *IEEE Transactions on Transportation Electrification*, vol. 8, no. 4, pp. 4378–4390, Dec. 2022.
- [11] H. Zhang and A. Wu, "Common-Mode Noise Reduction by Parasitic Capacitance Cancellation in the Three-Phase Inverter," *IEEE Trans Electromagn. Compat.*, vol. 61, no. 1, pp. 295–300, 2019.
- [12] Z. Zhang, L. Wei, P. Yi, Y. Cui, P. S. Murthy, and A. M. Bazzi, "Conducted Emissions Suppression of Active Front End (AFE) Drive Based on Random Switching Frequency PWM," *IEEE Trans Ind. Appl.*, vol. 56, no. 6, pp. 6598–6607, Nov. 2020.
- [13] D. Muller, M. Beltle, and S. Tenbohlen, "EMI Suppression of a DC-DC Converter Using Predictive Pulsed Compensation," *IEEE Trans Electromagn. Compat.*, vol. 63, no. 6, pp. 2134–2142, Dec. 2021.
- [14] H. Loschi, R. Smolenski, P. Lezynski, D. Nascimento, and G. Demidova, "Aggregated conducted electromagnetic interference generated by DC/DC converters with deterministic and random modulation," *Energies (Basel)*, vol. 13, no. 14, Jul. 2020.
- [15] P. Lezynski, R. Smolenski, H. Loschi, D. Thomas, and N. Moonen, "A novel method for EMI evaluation in random modulated power electronic converters," *Measurement (Lond)*, vol. 151, p. 107098, 2020.
- [16] Q. Ji, X. Ruan, M. Xu, and F. Yang, "Effect of duty cycle on common mode conducted noise of DC-DC converters," *2009 IEEE Energy Conversion Congress and Exposition, ECCE 2009*, 2009.
- [17] M. I. Sudrajat, M. A. Wibisono, N. Moonen, and F. Leferink, "Conducted Emission of a DC Motor Speed Drive: an Approach on Risk Assessment for Ship Application," in *2023 IEEE 7th Global Electromagnetic Compatibility Conference, GEMCCON 2023*, Institute of Electrical and Electronics Engineers Inc., 2023, pp. 54–55.
- [18] R. Smolenski, P. Lezynski, J. Bojarski, W. Drozd, and L. C. Long, "Electromagnetic compatibility assessment in multiconverter power systems – Conducted interference issues," *Measurement (Lond)*, vol. 165, p. 108119, 2020.
- [19] D. Apablaza and J. Muñoz, "Laboratory Implementation of a Boost Interleaved Converter for PV Applications," *IEEE LATIN AMERICA TRANSACTIONS*, vol. 14, no. 6, pp. 2738–2743, 2016.
- [20] K. Niewiadomski, R. Smolenski, P. Lezynski, J. Bojarski, D. W. P. Thomas, and F. Blaabjerg, "Comparative Analysis of Deterministic and Random Modulations Based on Mathematical Models of Transmission Errors in Series Communication," *IEEE Trans Power Electron*, vol. 37, no. 10, pp. 11985–11995, Oct. 2022.